Geodynamics, thermal structure and depth of the brittle and semi-brittle layers in the Northern Apennine (Italy)

F. Mongelli[1], G. Minelli[2] and M. Loddo[1]

[1] *Dipartimento di Geologia e Geofisica, Università di Bari, Italy*
[2] *Dipartimento di Scienze della Terra, Università di Perugia, Italy*

(Received May 16, 2005; accepted December 21, 2005)

ABSTRACT. The Northern Apennines are the exposed part of an accretionary prism which was formed as a result of the westward subduction of the continental Adria microplate. This prism occurred during two phases: the first between 11.2 and 5.3 Ma ago and the second from 3.6 Ma onwards, due to the stacking of continental upper crust strata, scraped off during the subduction. A 1D physical-mathematical model has been elaborated to compute the effect of tectonic stacking of the mantle and the radioactive components of the heat flow. The heat contribution, which resulted from the friction between the strata, has also been calculated. We find that the cooling effect of the thrusting is almost compensated by the heating by friction, so that the undisturbed surface geothermal gradient 29 ± 0.3°C km^{-1} of the Adriatic lithosphere is reduced to 24.5°C km^{-1} at the outcropping sector of the thrust. This agrees with the gradient 27°C km^{-1} ± 15% observed in deep oil wells. As a consequence of the thrusting, it has been found that, in particular, the 300°C and 450°C isotherms which in the stable Adriatic lithosphere are located at 13.2 and 24.8 km respectively, and delimit the semi-brittle layer separating the brittle upper layer from the deeper ductile one, are located at different depths in the Apennines. In fact, the upper limit is located at about 11 km depth, while the deep limit is located at about 50 km depth. Then, the seismically more active brittle layer and the semi-brittle are thicker and deeper.

1. Introduction

The central-northern Apennines are an area characterized by intense seismic activity, which peaked with the September – October 1997 sequence: the magnitude of the major earthquakes reached 4.9 – 5.9 (Amato *et al.*, 1998).

The depth of the hypocentres is generally about 10 km, but ipocentres at a depth of more than 40 km have been observed (Morelli *et al.*, 2000; Tallarico *et al.*, 2005).

Seismological observations suggest that earthquakes tend to nucleate in proximity of the base of the brittle zone while, in some instances, the rupture suggests propagation deeper into the so-called semi-brittle zone (Scholtz, 1988, 1990). In a quarz-feldspathic crust, this zone is typically comprised between 300°C, marking the transition of the behaviour of quartz from brittle to ductile, and 450°C, the equivalent limit for feldspar. Although these temperatures are not absolute, they are nevertheless indicative.

The position of a brittle and a semi-brittle layer is essential for the rheology calculation of the lithosphere (Dragoni *et al.*, 1997).

The temperature distribution, in turn, strongly depends on the geological history of the region. For instance, Dragoni *et al.* (1996) compared stresses in two geodynamically different areas of Italy using appropriate geotherms: stable foreland (Apulian plate) and extensional back-arc (Tuscan basin); they suggest that in areas that are characterized by a very high temperature gradient, as in Tuscany ($G \geq 50$°C km^{-1}), subcrustal seismicity is not to be expected; indeed, this result is confirmed by the absence of events deeper than 20 km.

A previous study on the thermal state of the Apennine chain was carried out by Mongelli *et al.* (1989). Significant improvements about the structure of the orogenic chain have been obtained since than. Moreover, Mongelli *et al.* (1989) did not consider the rock radioactivity. At present, the results of the CROP 03 seismic profile crossing the chain sheds new light on the geological structure.

In this paper, we calculate separately the effect of the thrust on the mantle and radioactive components of the heat flow of the stable slab, and the heat contribution by friction between the moving layers.

The aim of the present study is to recalculate the thermal state of a thrust region such as the Apennines, with the main purpose of calculating how the depths of the brittle and semi-brittle zone are modified by the thrusting.

2. Geodynamics of the Northern Apennines

From a geodynamic point of view, the Northern Apennine thrust belt is the exposed sector of an accretionary wedge related to the westward subduction of the Adria microplate. The subduction is largely supported by geological, geophysical and volcanological research (Mongelli *et al.*, 1975; Peccerillo, 1985; Royden *et al.*, 1987; Channel and Mareschal, 1989; Beccaluva *et al.*, 1989; Spakman, 1989; Doglioni, 1991; Amato *et al.*, 1993; Serri *et al.*, 1993; Castellarin *et al.*, 1994; Selvaggi and Chiarabba, 1995; Faccenna *et al.*, 1996; Piromallo and Morelli**,** 1997**;** and others). Moreover, a recent study by Lucente *et al.* (1999) confirmed the existence of a subduction plate by tomographic inversion down to 600 km. The CROP 03 deep seismic reflection line (Barchi *et al.*, 1988a, 1988b) shed some light on the geometry and the kinematics of the Northern Apennine accretionary wedge.

Taking into account that the westward subduction of the Adriatic plate has a rate of about 3 cm a^{-1} in the Calabrian arc and is about nul in the northernmost sector, we assume 1.0 – 1.5 cm a^{-1} for the central northern sector.

According to Doglioni *et al.* (1999a, 1999b), from east to west the accretionary prism is composed of stacked sectors of upper crust scraped-off the top of the subduction plate.

The Northern Apennine accretionary wedge began to develop during the Late Oligocene-Lower Miocene in a regime of collision between the already built Alpine chain and the Tuscan continental margin. The Umbria-Marche Apennine sector started to develop in the Late Burdigalian-Langhian times and its outer sector originated during late Miocene and Pliocene. This belt is still seismically active today (Amato and Selvaggi, 1991; Frepoli and Amato, 1997; Argnani, 1998).

Following previous stratigraphic-structural synthesis (Castellarin, 1994, 2001) and according to Barchi *et al.* (1988a, 1988b, and references therein), the age of the syntectonic turbidites

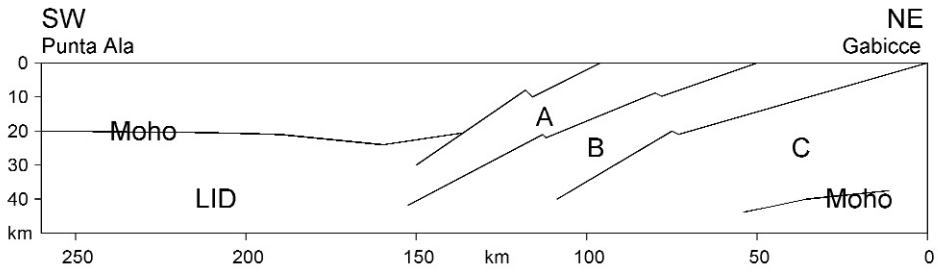

Fig. 1 - Schematic representation of the results of the deep seismic profile CROP 03 [after Barchi *et al.*, (1998a) and (1998b), simplified].

supports the general progression of the contractional events from west to east. In particular, the Tuscan turbidites of western Umbria (Falterona FM) were deposited in the Upper Oligocene (23.8 Ma) – Lowermost Miocene (20.3 Ma); the turbidites of the Umbria pre-Apennines (Marly-Sandstone Fm) are from the Upper Burdigalian (16.4 Ma) to the Lower Tortonian (11.2 Ma); the turbidites of the Inner Marche basins range from the Upper Serravallian (11.1 Ma) to the Messinian (5.3 Ma). Finally, the turbidites of the outer Marche foredeep date from the Late Pliocene (3.6 Ma) onward.

Fig. 1 is a schematized representation of the CROP 03 profile, within the area extending from Tuscany to the Adriatic shore line. The progressive stacking from west to east of the Adriatic continental crust occurs by means of two main thrusts during periods of time that can be estimated on the basis of the age of sintectonic terrigenous sediment (Barchi *et al.*, 1988a, 1988b, and references therein). The thrusting of unit A over unit B is associated with the terrigenous succession that was deposited in the inner Marche region during Tortonian - Messinian between about 11.2 Ma and 5.3 Ma. Successively, the thrusting of units A+B over C could be in relation to the Pliocene-Quaternary terrigenous units, deposited in the outer Marche domain and in the adjoining Adriatic foredeep, from 3.6 Ma to the present.

We assume that each A-B sector has a thickness of 15 km and is composed of about 6 km of terrigenic, carbonatic and evaporitic successions and 9 km of basement, according to Barchi *et al.* (1988a, 1988b, and references therein) and Anelli *et al.* (1994).

According to Doglioni *et al.* (1998), and Barchi *et al.* (1998a, 1998b), the stacking of the crustal elements is related to the Adriatic slab roll-back (Fig. 2).

Within this framework, the crustal extension and the extensional earthquakes at the western side of the chain (Barchi *et al.*, 1988a, 1988b; Boncio *et al.*, 1998; Collettini *et al.*, 2000) may be the result of the uprising astenospheric wedge (Fig. 2) that causes the uplift of the area (Doglioni, 1991; Doglioni *et al.*, 1999a, 1999b).

The following model (Fig. 3) is proposed in the attempt to evaluate the thermal aspects of the phenomenon:

- from 11.2 Ma to 5.3 Ma ago, unit A overthrusts unit B, while the subduction proceeds;
- from 3.6 Ma ago to present, unit A+B overthrusts unit C.

As the accretionary prism stacking occurs at the same time as the rollback, the package is

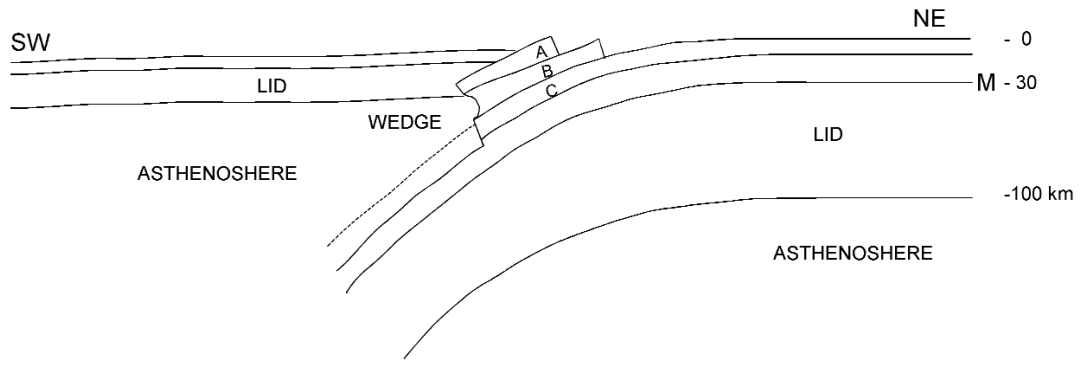

Fig. 2 - Geodynamic model of the Adriatic plate subduction.

always over a constant dip sector of the lithosphere (Fig. 3).

3. The stable Adriatic plate geotherm

The thermal conditions of the Adriatic plate, which has not yet been involved in the subduction process, provides the non-disturbed geotherm before the thrusting (i.e. the stable reference geotherm).

According to gravimetric, seismic and seismological studies (Locardi and Nicolich, 1988 and

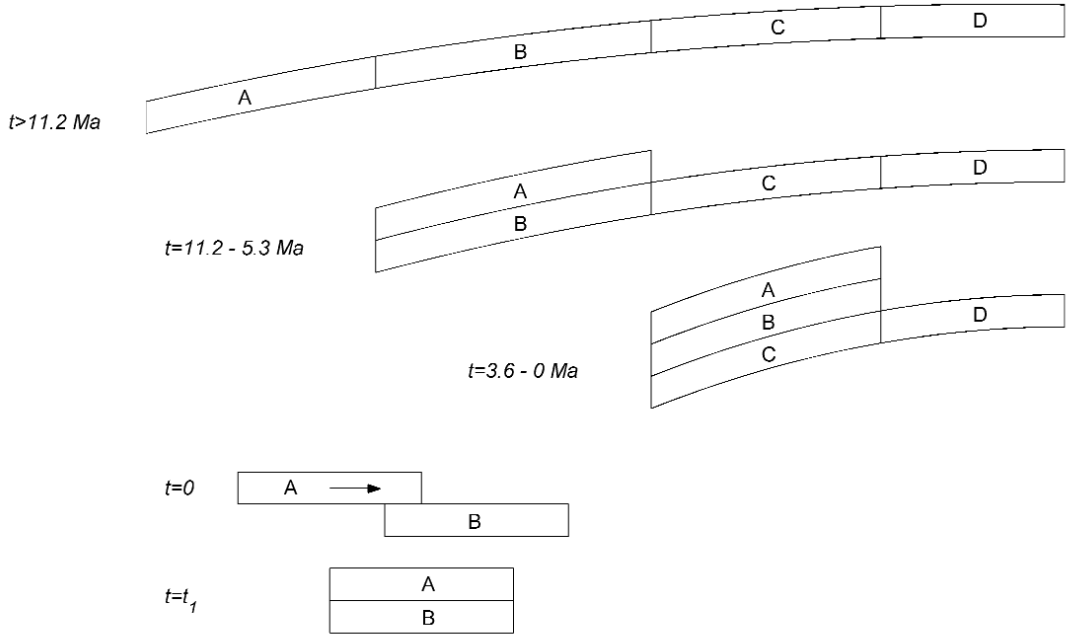

Fig. 3 - Simplified sketch of the thrusting of sediments.

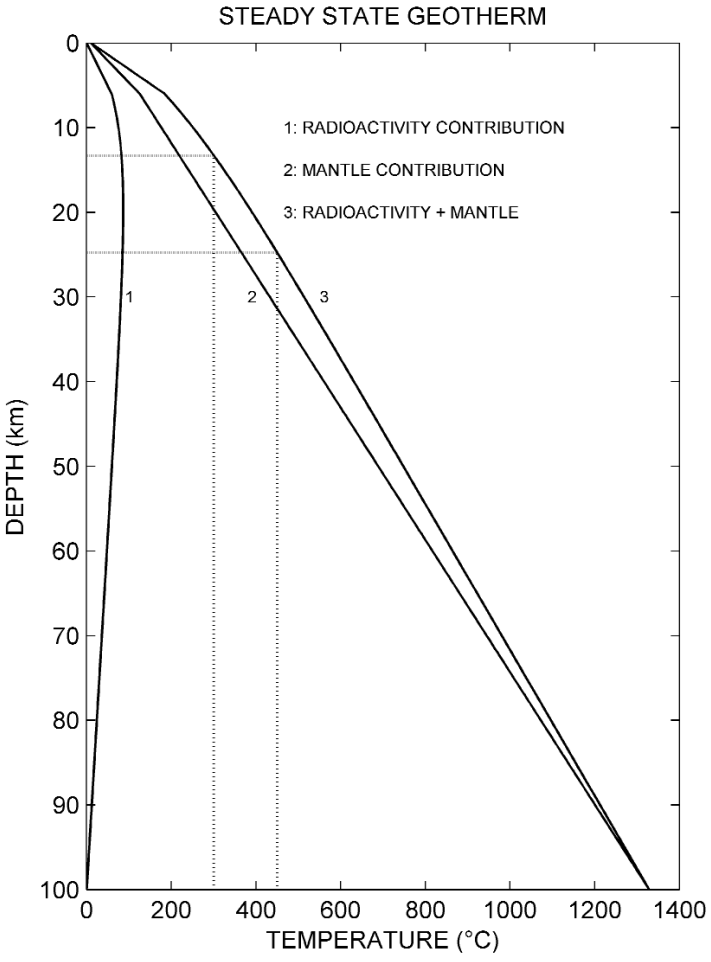

Fig. 4 - Steady state geotherm of the stable Adriatic plate.

references therein; Panza *et al.*, 2003) the Adriatic plate is characterised by:

a shallow layer H_1 of sediments about 6 km thick;

a Moho, at a depth of 30 km;

a total L_1 thickness of about 100 km.

In Apulia, which is the southern outcropping sector of the Adriatic plate, the thermal gradient at the surface, corrected for climatic change, and the conductivity are respectively (Mongelli and Pagliarulo, 1997; Loddo and Mongelli, 2005):

$$G_0 = 29.0 \pm 0.3 °C\,km^{-1},\ \lambda_s = 2.0 \pm 0.2 Wm^{-1} °K^{-1},$$

and by using the error propagation relation the heat flow is:

$$q_0 = 58 \pm 5.2 mWm^{-2}.$$

For the northern Adriatic Sea, Della Vedova *et al.* (2001), from deep offshore temperatures, corrected for bathymetry, paleoclimate and sedimentation, obtained a mean value of about 60 mW m-^{2}.

Let's assume:

$$\begin{aligned} q_0 &= q_{0m} + q_{0r}, \\ G_0 &= G_{0m} + G_{0r}, \end{aligned} \qquad (1)$$

where the subscript *m* and *r* indicate the sublithospheric mantle and radioactive contributions, respectively. Assuming the surface temperature to be T_0 =10°C; and the lithosphere base temperature to be T_a =1330°C, the lithospheric average thermal gradient of mantle origin is obtained:

$$\bar{G}_{0m} = \frac{T_a - T_0}{L_1} = 13.2 °\mathrm{C\,km^{-1}}.$$

Supposing a thermal conductivity λ_s = 2 Wm^{-1}°C^{-1} for the sedimentary thickness H_1 (mainly limestones) and λ_T= 3 Wm^{-1}°C^{-1} [averaged conductivities of granite and basic rocks of the crust and ultrabasic rocks of the mantle, decreasing with temperature (Zoth and Hänel; 1988)] for the remaining lithosphere, at the discontinuity between the sedimentary layer and the remaining lithosphere we have:

$$\begin{aligned} \lambda_s G_{ms} &= \lambda_r G_{mr}, \\ G_{mr} &= 0.67 G_{ms}, \end{aligned}$$

where G_{ms} = G_{0m} and G_{mr} represent the gradients of mantle origin in the second layer. The following relation holds:

$$T_0 + H_1 G_{ms} + (L_1 - H_1) G_{mr} = T_0 + 13.2 \cdot 100\ °C,$$

from which G_{ms} = 19.2°C km^{-1} and G_{mr} = 12.8°C km^{-1} result.

Since G_{ms} = G_{0m} and G_0 = 29.0°C km^{-1}, the following is obtained:

$$\begin{aligned} G_{0m} &= 19.2 °\mathrm{C\,km^{-1}}, \quad & q_{0m} &= 38.4\ \mathrm{mW\,m^{-2}}, \\ G_{0r} &= 9.8 °\mathrm{C\,km^{-1}}, \quad & q_{0r} &= 19.6\ \mathrm{mW\,m^{-2}}, \end{aligned}$$

Therefore, the mantle contribution to the geotherm is:

$$\begin{aligned} T_m &= T_0 + G_{0m} z, && 0 \le z \le H_1, \\ T_m &= T_0 + G_{0m} H_1 + G_{mr}\left(z - H_1\right), && H_1 \le z \le L_1. \end{aligned} \qquad (2)$$

The radioactive contribution is calculated on the basis of the equation:

$$\frac{d^2T}{dz^2} = -\frac{A(z)}{\lambda}, \tag{3}$$

where $A(z)(\mu\text{W m}^{-3})$ represents the heat productivity of radioactive origin. Let assume $A_S = 0$ in the sedimentary layer of thickness H_1, since the limestones of the Adriatic plate are radioactive nuclei free (P. Gasparini, pers. com.) and:

$$A(z) = A_0 \exp\left[-(z - H_1)/D\right], \tag{4}$$

(Lachenbruch, 1970) in the remaining lithosphere. D is the radioactive length scale.

Eq. (3) may be split into:

$$\begin{aligned} &\frac{d^2T}{dz^2} = 0, && 0 \le z < H_1, \\ &\frac{d^2T}{d(z - H_1)^2} = -\frac{A_0}{\lambda_r}\exp\left[-(z - H_1)/D\right], && H_1 \le z \le L_1, \end{aligned} \tag{5}$$

with boundary conditions:

$$\begin{aligned} &T(z = 0) = 0, \\ &T(z = L_1) = 0, \\ &T(z = H_1^+) = T(z = H_1^-). \end{aligned}$$

The following is obtained:

$$T_r = \left(\frac{dT_r}{dz}\right)_{z=0} \cdot z = G_{0r} \cdot z, \qquad 0 \le z < H_1, \tag{6}$$

and

$$\begin{aligned} T_r(z) = {} & G_{0r}H_1 + \frac{A_0}{\lambda_r}D^2\left[1 - \exp\left(-\frac{z - H_1}{D}\right)\right] + \\ & - \left\{\frac{G_{0r}H_1}{L_1 - H_1} + \frac{A_0}{\lambda_r(L_1 - H_1)}D^2\left[1 - \exp\left(-\frac{L_1 - H_1}{D}\right)\right]\right\}(z - H_1), \quad H_1 \le z \le L_1. \end{aligned} \tag{7}$$

Ultimately, the stable geotherm is given by:

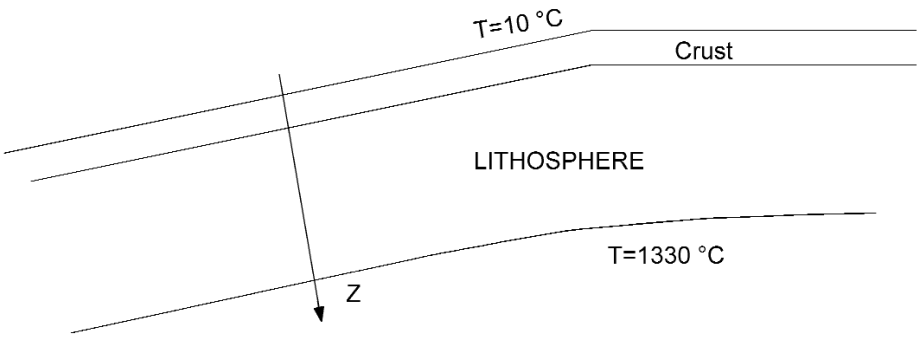

Fig. 5 - Reference system for the geodynamic model.

$$T(z) = T_m(z) + T_r(z).$$

We assume $A_0 = 2.5\ \mu\mathrm{W\,m^{-3}}$, $D = 8$ km (Rybach, 1988).

Fig. 4 shows the mantle, radioactive and total geotherm. The main contribution is supplied by the mantle. The discontinuity at a depth of 6 km is due to the conductivity variation and increase in radioactive productivity.

The semi-brittle layer comprised between 300°C and 450°C is located between 13.2 and 24.8 km.

4. Thrust geotherm

The thermal evolution of thrusts have been investigated by various authors (Oxburg and Turcotte, 1974; Bickle *et al.*, 1975; England, 1978; Brewer, 1981; Molnar *et al.*, 1983; Mongelli *et al.*, 1989; England and Molnar, 1990; Cermak and Bodri, 1996; and others).

Lithospheric convergence occurs at a rate of a few cm/a. Consequently, heat transfer has both a conductive and advective component. Molnar and England (1990) have studied this problem under a stationary regime. However, if the movement occurred long ago and/or very rapidly and was of short duration, it is reasonable to consider the movement, as many authors have done, as being instantaneous. Also in the case of the Northern Apennine, where the thrusts were recent and of short duration, for sake of simplicity, we assume these as instantaneous at the mean time between the beginning and the end, that is 8.55 Ma and 1.8 Ma of each thrust. Consequently, it will be necessary to consider the consequence of such an assumption.

From a geothermal point of view, the Apennine thrusting presents another aspect. As we can see in Fig. 2, the upper sector of the thrust is outcropping and the lower sector is buried. This last sector is mainly warmed by the adjacent hot Tuscan basin, while the influence on the far upper sector is lesser.

The present study, in accordance with the geodynamic model proposed, considers the subducted lithosphere as a reference and the temperature at the lithosphere base as constant in

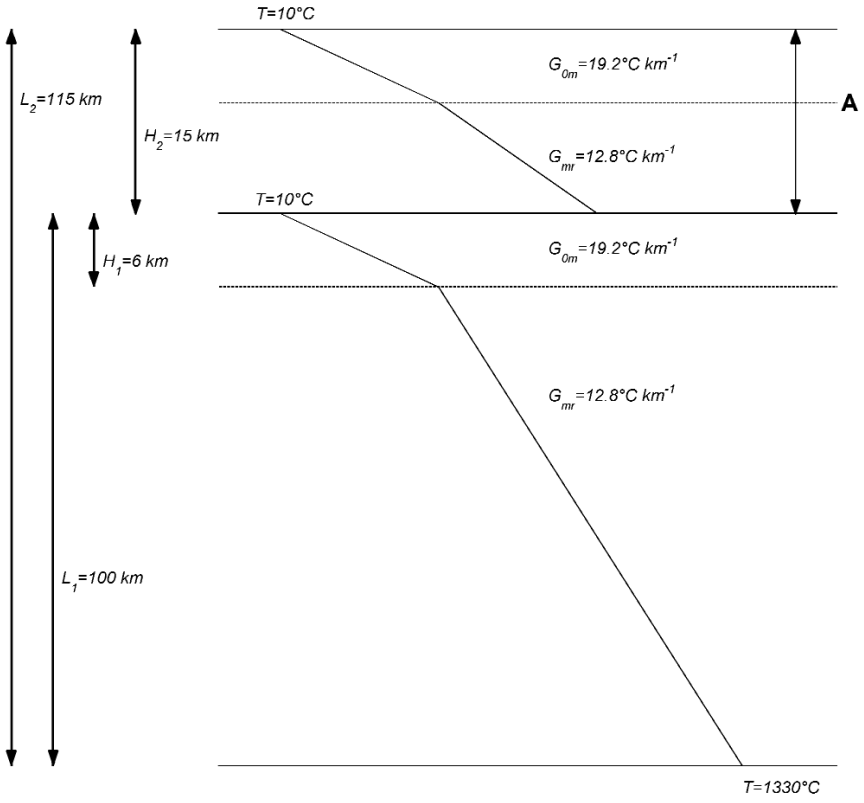

Fig. 6 - Sketch of the first thrust and temperature mantle component.

time (Fig. 5). The lateral contribution of heat is at the moment disregarded, but will be discussed later.

Furthermore, for the sake of simplifying the problem, the lithosphere surface has been considered as a plane.

The temperature distribution, following thrusting, depends on three different processes:

1. the variation of heat contribution of mantellic origin, as a result of lithospheric thickening;

2. the variation of heat contribution of radioactive origin, as a result of the vertical distribution variation of radioactive rocks;

3. the heat contribution resulting from the friction between the scraped-off sectors of the crust and the basement.

The one-dimension heat conduction equation is:

$$\frac{\partial^2 T}{\partial z^2} + \frac{A(z)}{\lambda} = \frac{1}{k}\frac{\partial T}{\partial t}\,, \tag{8}$$

where z is perpendicular to the lithosphere boundaries and directed inwards, T (°C) is the

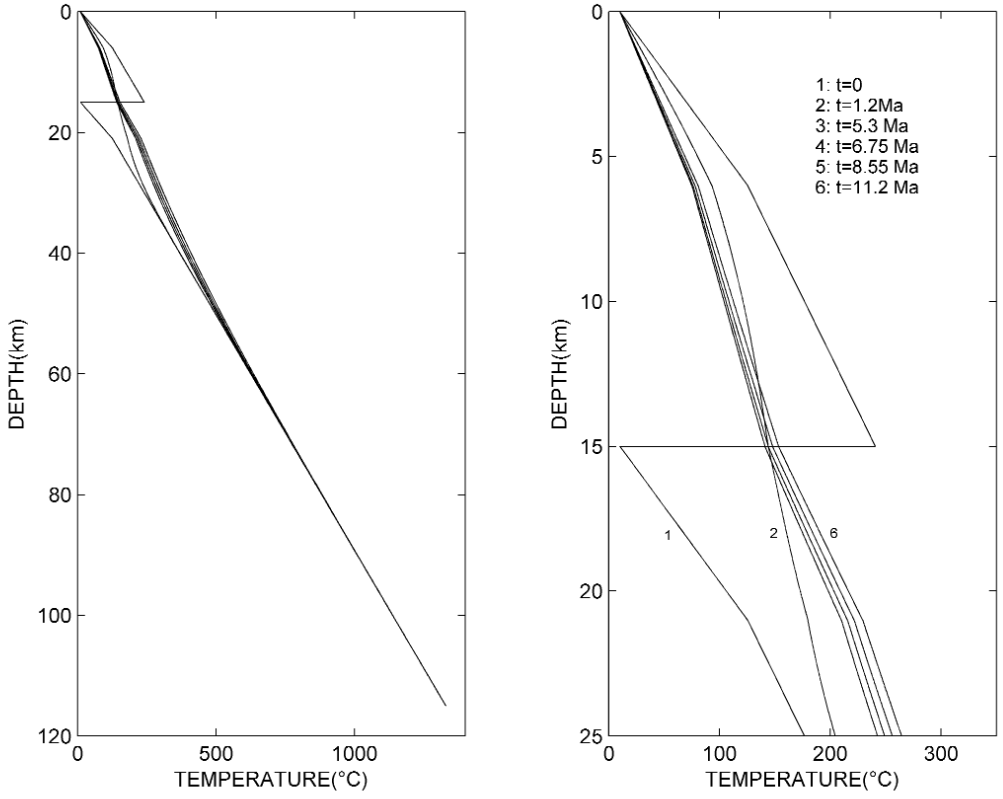

Fig. 7 - Mantle geotherm evolution after the first thrust.

temperature, $A\ (\mu \mathrm{W\ m^{-3}})$ is the heat productivity of the radioactive rocks, $k\ (\mathrm{m^{-2}\ s^{-1}})$ is the thermal diffusivity and λ is the thermal conductivity of the rocks.

As the heat flow equation is linear, the different processes have been considered separately (see Molnar *et al.*, 1983).

4.1. Mantle contribution variation

4.1.1. First thrust effect

From 11.2 Ma ago (assumed as t=0) to 5.3 Ma ago a crustal block A, having a thickness H_2, a temperature equal to that of the layer H_2 of the lithosphere and the same average diffusivity, overthrusts a lithosphere having thickness L_1 and temperature mantle T_m, given by Eq. (2). Thus, a structure is built whereby the total thickness is $L_2 = L_1+H_2$ (Fig. 6). The solution to Eq. (8) with $A\ (z) = 0$ as well as the resulting gradient has been obtained by numerical methods.

Fig. 7 shows the geotherms obtained for $G_{0m} = 19.2°\ C\ \mathrm{km^{-1}}$; $G_{mr} = 12.8°\ C\ \mathrm{km^{-1}}$, $H_2 = 15$ km, $H_1 = 6$ km, $L_2 = 115$ km and $k = 31.54\ \mathrm{km^2\ Ma^{-1}}$. The initial saw-tooth trend disappears after 1.2 Ma, while the discontinuity at a depth of 21 km remains stable. This is due to the conductivity variation. After 1.2 Ma the temperature increases steadily throughout the entire structure to a point of quasi-stationary regime. Moreover, the temperature differences between the geotherm relative the mean time (8.55 Ma) and those relative the initial (11.2 Ma) and the final time (5.3

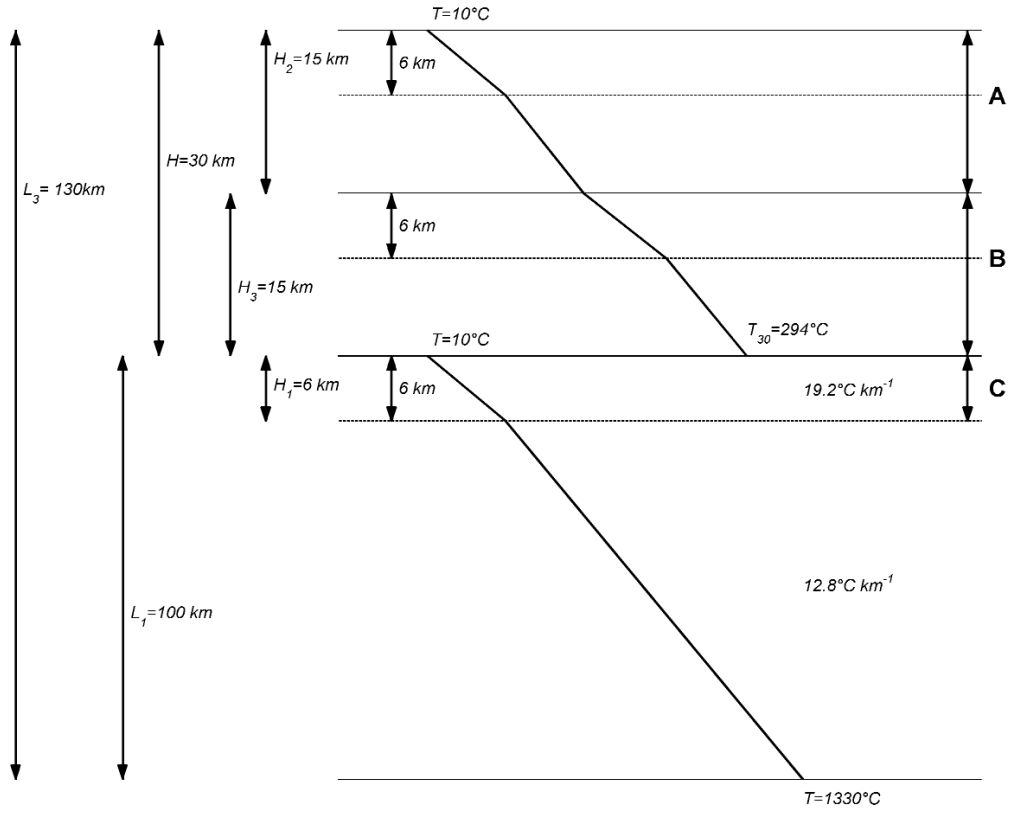

Fig. 8 - Sketch of the second thrust and temperature mantle component.

Ma) of the thrust, are variable from zero at surface to 5-10°C at a depth of 21 km. This means that the assumption of the mean time of the thrusting does not give significant error.

4.1.2. Second thrust effect

We suppose that at t=1.8 Ma ago the block layers A+B, having a thickness of $H=H_2+H_3$ as a product of the preceding thrust, overthrusts the undisturbed lithosphere of thickness L_1. A new structure with a total thickness $L_3=L_1+H_2+H_3$ (Fig. 8) develops.

While the temperature of mantle origin in lithosphere L_1 is the undisturbed one, the temperature distribution in the overthrust sector at time 8.55-1.8=6.75 Ma is represented by curve 4 of Fig. 7. The solution to the problem has been obtained by numerical methods. Fig. 9 represents the geotherm evolution through time for H_3=15 km, L_3=130 km. Once again, the saw-tooth trend disappears rapidly, whereas the discontinuity at 36 km is maintained owing to the conductivity variation.

The curves obtained for t=0.1, 1.8, 3.6 Ma are very different. Hence, it is impossible to assume an unique time for all the thrust.

Anyway, curve 2 (t=0.1 Ma) may represent the geotherm at the outcropping sector of the

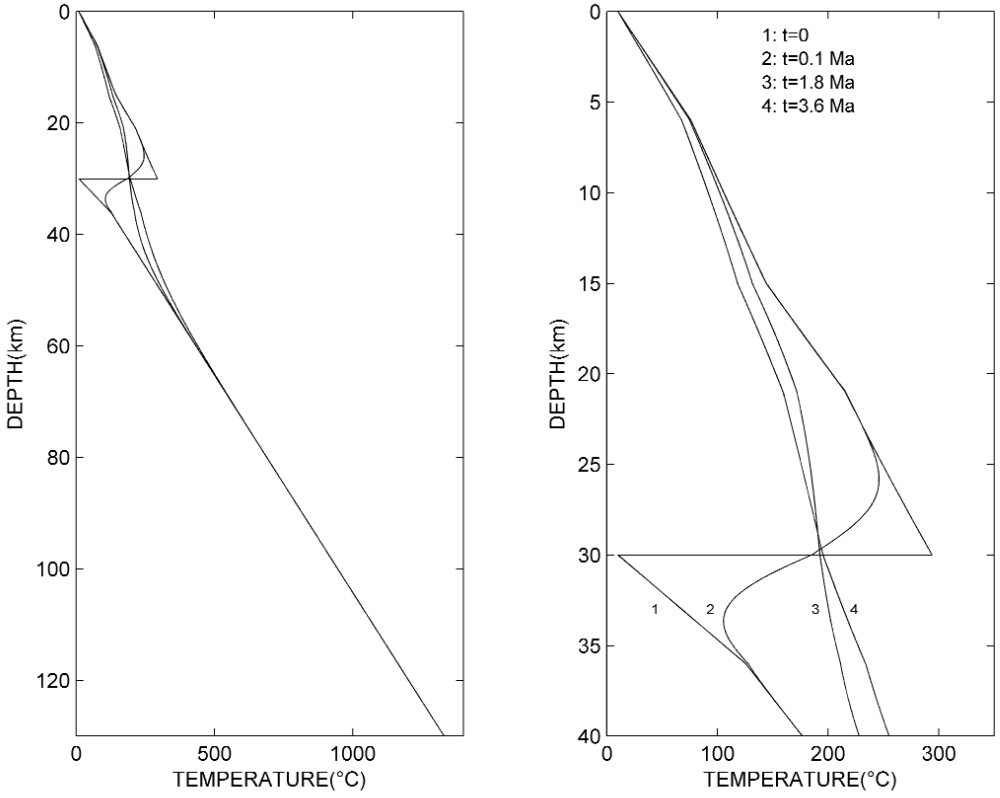

Fig. 9 - Mantle geotherm evolution after the second thrust.

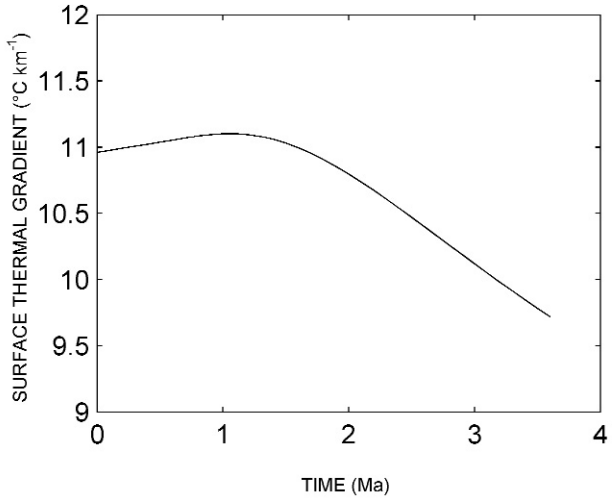

Fig. 10 - Evolution of the surface gradient of the mantle component after the second thrust.

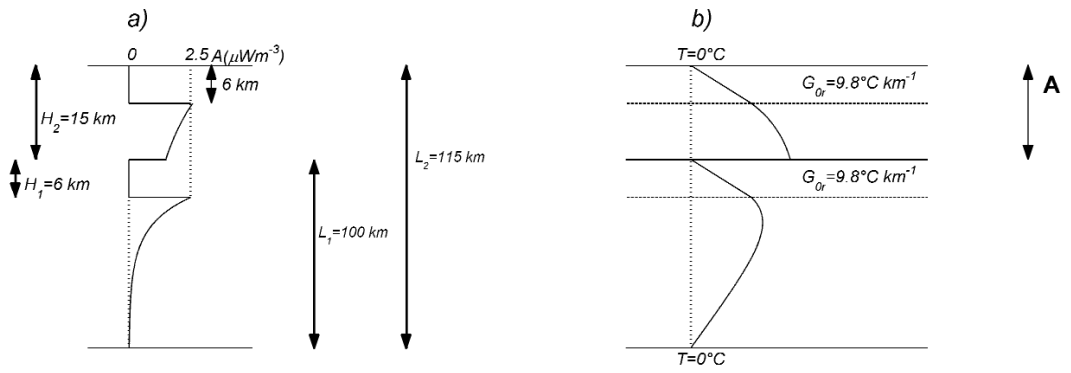

Fig. 11 - Sketch of the first thrust: distribution of rock radioactivity; distribution of initial temperature.

Apennine chain, where the thrusting arrives just. In the first 30 km, the temperature distribution is that of the first thrust, at time 6.75 Ma.

Fig. 10 shows the surface geothermal gradient evolution through time. Starting from 10.9°C km^{-1} at t=0, after a little increase to 11.1°C km^{-1} at 1.2 Ma, it decreases rapidly to 9.8°C km^{-1} at 3.6 Ma. Values at t=0 (10.9°C km^{-1}) may represent the surface gradient at present, at the outcropping sector of the double thrust.

4.2. Radiogenic contribution variation

4.2.1. First thrust effect

At the instant t=0, the lithosphere of thickness L_1 presents, in its sedimentary body H_1, a heat productivity A_s=0 and a temperature given by Eq. (6), while, in the remaining lithosphere, a productivity given by Eq. (3a) and a temperature given by Eq. (7). A crustal sector H_2=15 km having productivity A_s=0 and temperature given by Eq. (6) in the first sedimentary 6 km, and a productivity given by Eq. (3a) and temperature given by Eq. (7) in the remaining 9 km, overthrusts the lithosphere (Fig. 11).

The solutions are obtained by numerical methods with the aforesaid initial conditions and the boundary conditions T=0 at z=0 and z=L_2=L_1+H_2, for the same parameter values previously used. As shown in Fig. 12, once again, the saw-tooth trend disappears after roughly 1 Ma. Furthermore, after 1-2 Ma the variations are rapid and then become very slow. In addition, the discontinuity, at a depth of 21 km, is evident.

4.2.2. Second thrust effect

Let us suppose that at t=1.8 Ma the block A+B (see Fig. 3) of thickness H_2+H_3=30 km overthrusts the undisturbed lithosphere of thickness L_1. In the block B=15 km the productivity is equal to that of block A (Fig. 13).

In the lithosphere L_1, the temperature of radioactive origin is the undisturbed one, whereas, in the overthrust sector H_2+H_3=H the temperature at time 8.55-1.8 =6.75 Ma is represented by curve 4 of Fig.12.

The thermal evolution is obtained by numerical methods with the aforesaid initial conditions

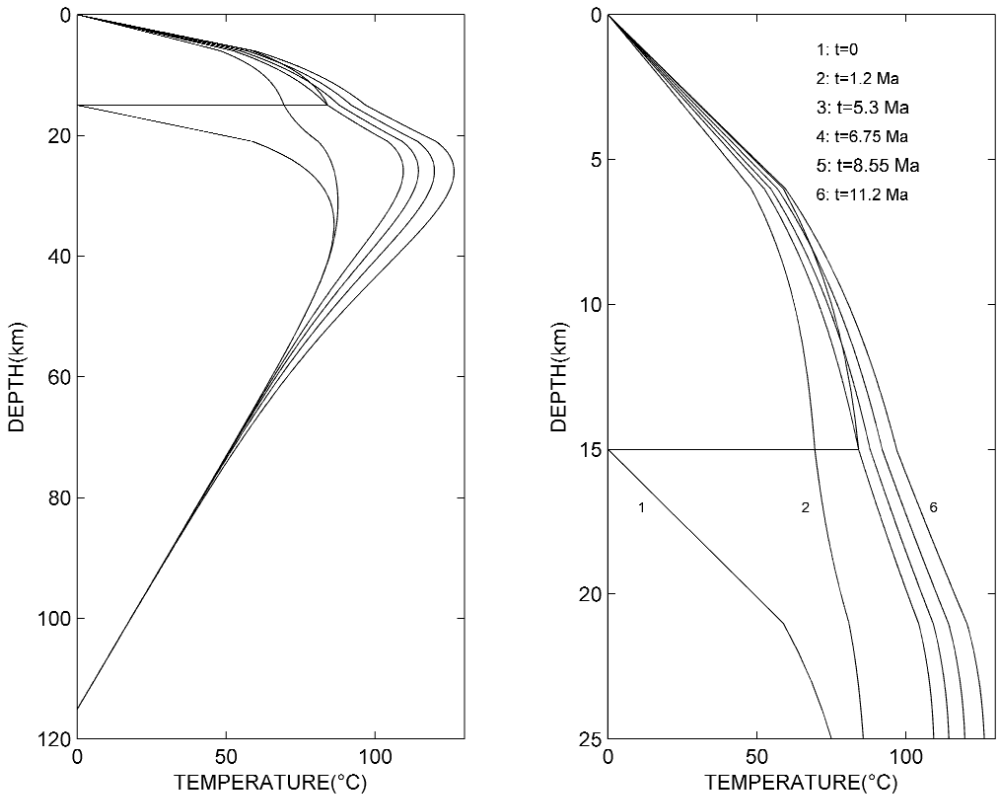

Fig. 12 - Evolution of the temperature of the rock radioactivity component after the first thrust.

and the boundary conditions T=0 at z=0 and z=L_3=L_1+H_2+H_3.

Fig. 14, represents the temperatures calculated by using the parameter values previously utilized. Once again, the saw-tooth disappears rapidly whereas the discontinuity at 36 km is maintained. The curves obtained are very different from each other.

Anyway, curve 2 (t=0.1 Ma) may represent the geotherm at the outcropping sector of the

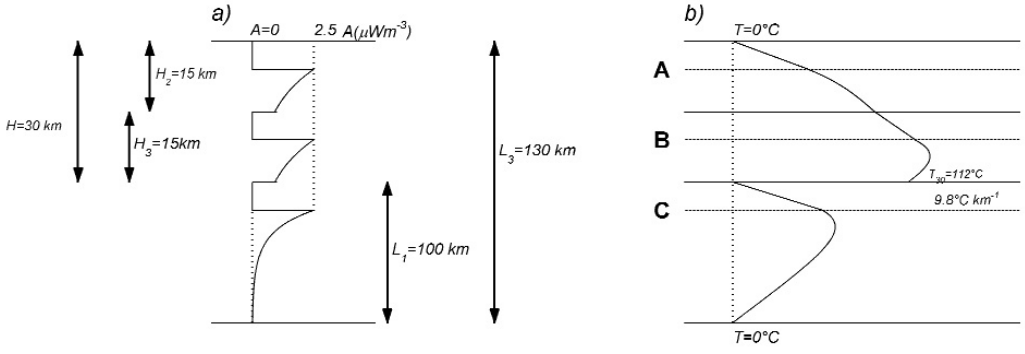

Fig. 13 - Sketch of the second thrust: distribution of rock radioactivity; distribution of initial temperature.

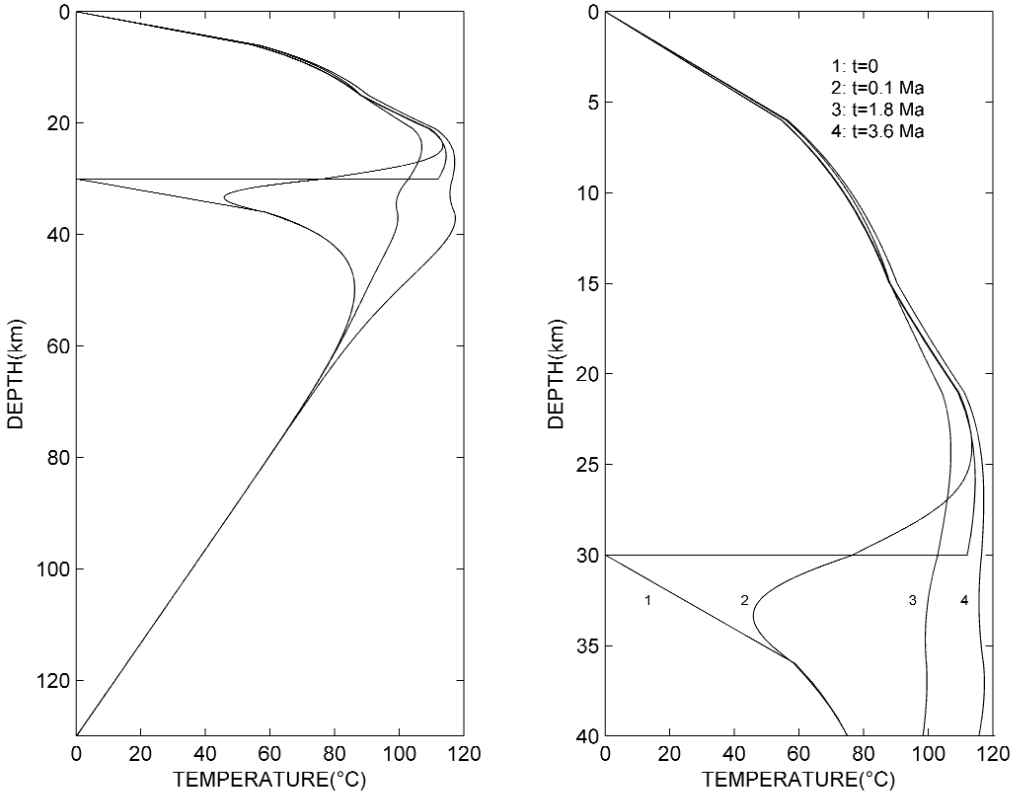

Fig. 14 - Evolution of the temperature of the rock radioactivity component after the second thrust.

Apennine chain, where the thrusting arrives just. In the first 30 km the temperature distribution is that of the first thrust, at time 6.75 Ma.

Fig. 15 shows the surface geothermal gradient evolution through time. Starting from 9.05°C km^{-1} at t=0 it increases rapidly to about 9.3°C km^{-1} at t=1.5 Ma, then it increases slowly to 9.4°C km^{-1} at t=3.6 Ma. The value at t=0 (9.05°C km^{-1}) may represent the surface gradient at present, at the outcropping sector of the double thrust.

4.3. Heat contribution by friction

The problem of heat contribution resulting from friction has been investigated by various authors, using different analytical methodologies such as:

- the source method (Lachenbruch and Sass, 1980, 1992);
- the Green function method (McKenzie and Brune, 1972; Brewer, 1981);
- the Dirac function to represent heat development (Molnar *et al.*, 1983).

In the present study, the source method was adopted as best suits the case of the double thrust.

4.3.1. First thrust effect

The sliding surface of plate A of thickness H_2=15 km over the underlying medium may be

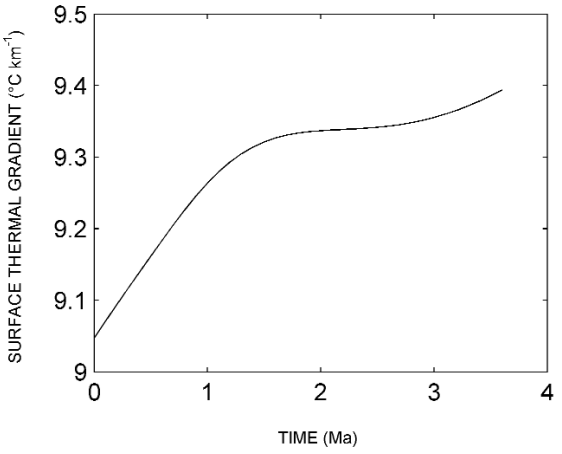

Fig. 15 - Evolution of the surface thermal gradient of the rock radioactivity component after the second thrust.

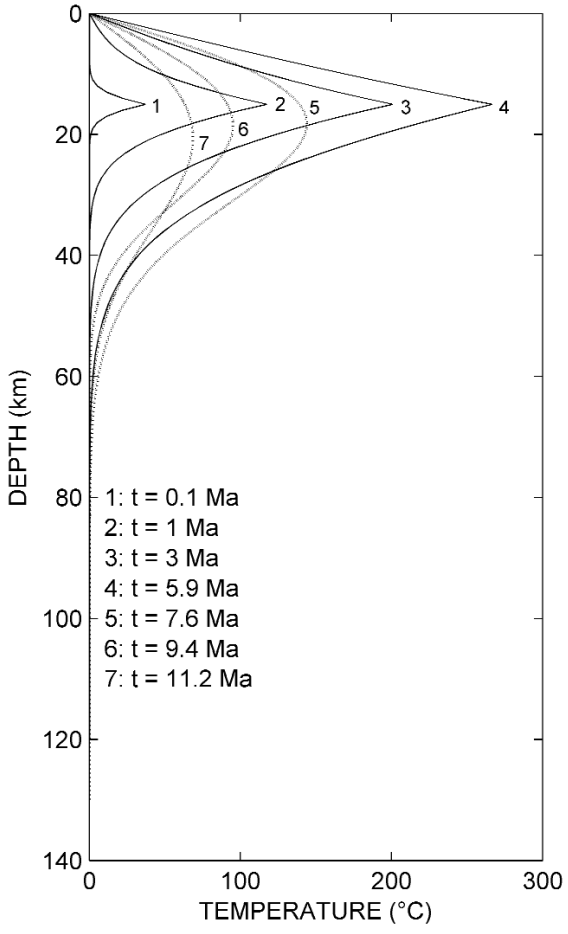

Fig. 16 - Decreasing of the thermal disturbance produced by friction after the first thrust.

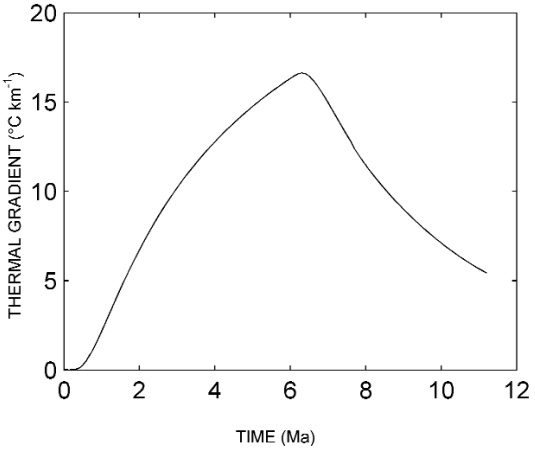

Fig. 17 - Evolution of the surface thermal gradient of the disturbance produced by friction after the first thrust.

considered as a continuous plane source which produces a quantity of heat per unit surface and unit time:

$$Q = v\tau,$$

where v is the sliding rate, τ is the shear stress, given by:

$$\tau = f\rho g H_2, \tag{15}$$

f is the dynamic friction coefficient, g the gravity acceleration, ρ the density of the overlying layer.

The thermal field produced by the plane source, as well as its image and relative thermal gradient, are calculated in Appendix.

We assume**:**

$$v = 1.5\ \mathrm{cm\,a^{-1}},\ g = 9.8\ \mathrm{m\,s^{-2}},\ \rho = 2650\ \mathrm{kg\,m^{-3}}.$$

Byerlee (1978) has shown from laboratory experiments on dry rock that above a pressure of 2 kbars (about 6 km depth) an upper limit to f is about 0.6 regardless of rock type.

Since the first sliding has a finite duration from 11.2 Ma to 5.3 Ma , it was necessary to superimpose a negative source of equal strength along its image, in order to obtain the thermal field after time 5.3 Ma. The temperature and gradient are calculated in the Appendix, taking also in account that at the time 7.6 Ma, when A+B overthrusts unit C at 3.6 Ma, the total thickness of the slab becomes 130 km.

Fig. 16 shows the increase of the temperature up to about 270°C during the sliding and the decrease after the sliding. We see that at present (curve 7) the thermal contribution by friction reduced to the maximum value of 70°C at a 21 km depth.

Fig. 17 shows the surface gradient variation throughout time. After an increas during the

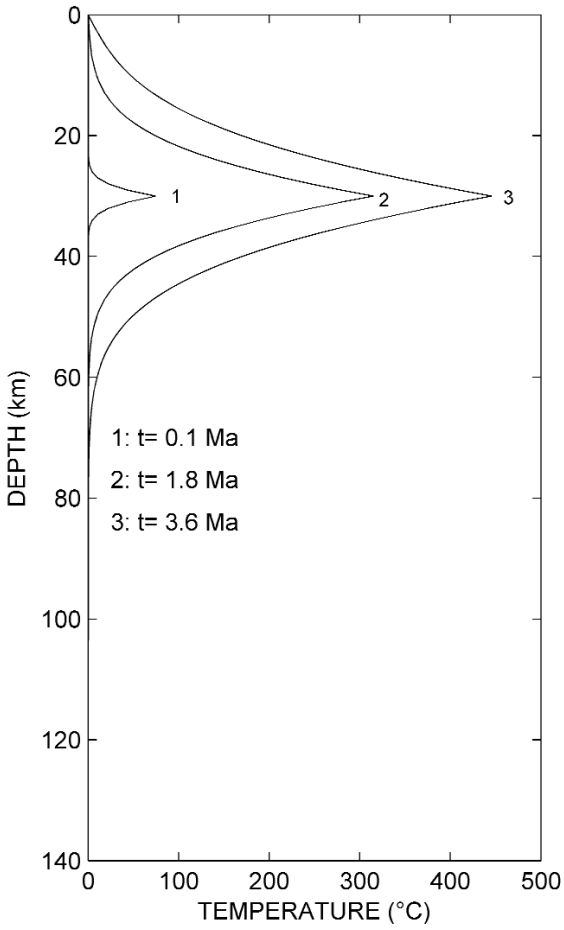

Fig. 18 - Increasing temperature disturbance produced by friction during the second thrust.

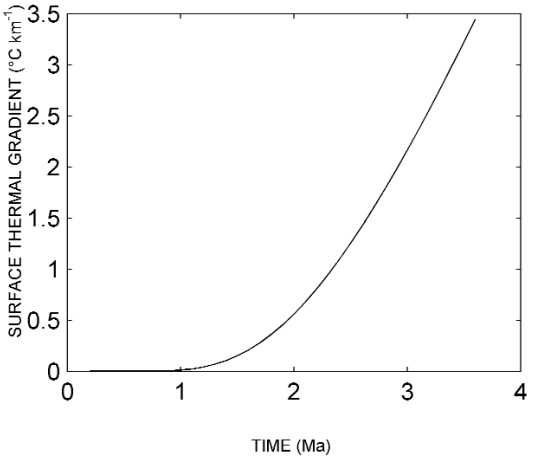

Fig. 19 - Evolution of the surface thermal gradient of the disturbance produced by friction after the second thrust.

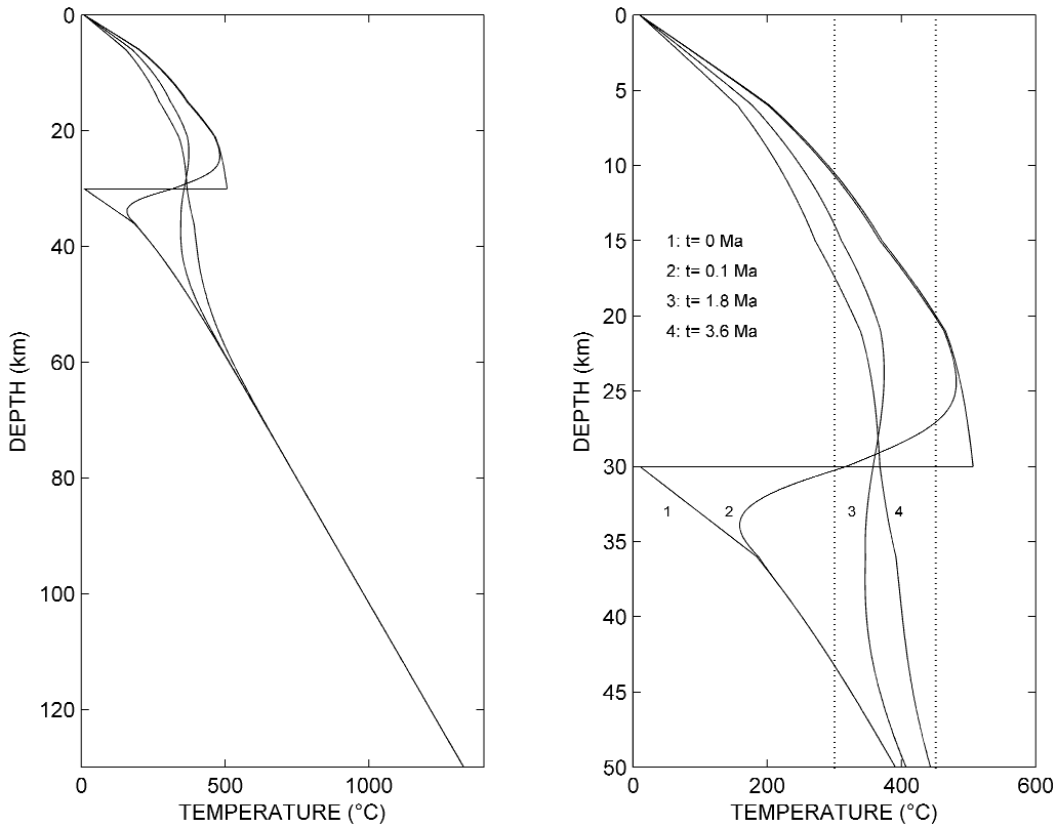

Fig. 20 - Evolution of the total surface geotherm (mantle + radioactivity + friction) from the beginning of the second thrust to the present.

sliding up to 16.8°C km^{-1}, after 6.5 Ma there is a decrease to about 5.5°C km^{-1} at the present time.

4.3.2. Second thrust effect

At a certain instant (3.6 Ma ago), the layer that had already doubled in thickness (H_2+H_3) begins to overthrust the undisturbed lithosphere. The shear stress is calculated as follows:

$$\tau = f\rho g\left(H_2 + H_3\right).$$

The thermal field and the gradient contribution are still expressed by the Appendix.

Fig. 18 shows the calculated temperatures. It may be observed that, at present, the strongest disturbance is about 450°C, at a depth of 30 km, while the temperature at time 0.1 Ma at the same depth is about 75°C.

As the slide moves from the depth to the surface, the outcropping sector of the building is involved only for a brief period. Then, the curve of 0.1 Ma may represent the situation in that sector.

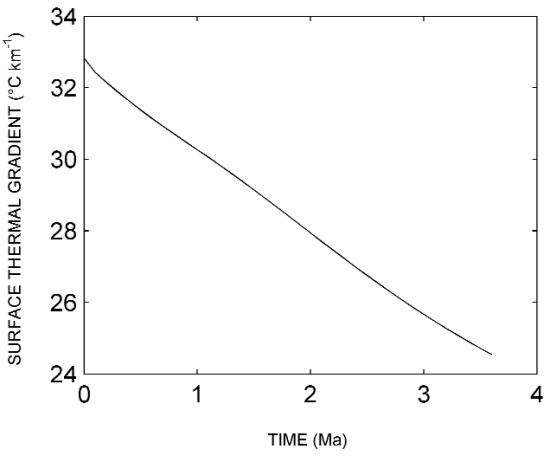

Fig. 21 - Evolution of the total geothermal gradient (mantle + radioactivity + friction) from the beginning of the second thrust to the present.

Fig. 19 shows the constant increase of the surface gradient. The strongest value is about 3.4°C km^{-1} at a time of 3.6 Ma, while at less than 0.2 Ma, representative of the outcropping, the gradient is nul .

4.4. Summing all the contributions

Fig. 20 shows the geotherms obtained by adding the contribution of the three thermal processes from 3.6 Ma ago to the present.

At present, the effect of the second thrust is dominant, because it is very recent.

Curves 1 and 2 represent the thermal situation of the outcropping sector of the double thrust presently.

Fig. 21 shows the variation of the surface thermal gradient through time. Starting from the value of about 33°C km^{-1} it decreases steadily to 24.5°C km^{-1} at 3.6 Ma. This trend depends on the fact that the second thrust of the buried sector is 3.6 Ma old, while the outcropping sector it arrives just and has an effect nul.

5. Conclusions

Our model entails approximations and semplifications with regards to physical, temporal, geometric parameters and neglects other geophysical influences. Anyway, the best test of our study is the comparison with experimental data. In fact, Della Vedova *et al.* (2001) studied four deep oil wells bored in mostly impermeable units of the Northern Apennines very far from Tuscan geothermal areas and obtained an average thermal gradient of 27±15%°C km^{-1} in good agreement with our calculated value for the outcropping sector of the thrust. The linearity of the observed temperatures demonstrates that the influence of the thermal disturbances, such as superficial effects, fluid motion, lateral heating, are negligible or compensate each other, thus confirming the validity of our model.

In conclusion, Fig.20 shows the depth of the semibrittle layer between the isotherms of 300 and 450°C. In particular, the isotherm of 300°C, which in the stable slab was at 13.2 km depth, at present is at about 11 km at the outcropping sector. The isotherm of 450°C, which in the stable slab was at 24.8 km, at present is at about a 50 km depth everywhere. As a consequence, the semibrittle layer and the depths of earthquake nucleation deepens and thicken.

Acknowledgements. The authors would like to thank two anonymous reviewers for their helpful comments and suggestions.

REFERENCES

Amato A., and Selvaggi G.; 1991: *Terremoti crostali e sub-crostali nell'Appennino Settentrionale*. Studi Geologici Camerti, **1**, 75-82.

Amato A., Alessandrini B., Cimini G.B., Frepoli A. and Selvaggi G.; 1993: *Active and remnant subducted slabs beneath Italy: evidence from seismic tomography and seismicity.* Annali di Geofisica, **36**, 201-214.

Amato A., Azzara R., Chiarabba C., Cimini G.B., Cocco M., Di Bona M., Margheriti L., Mazza S., Mele F., Selvaggi G., Basili A., Boschi E., Courboulex F., Deschamps A., Gaet S., Bittarelli G., Chiaraluce L., Piccinini G., and Ripepe M.,; 1998: *The 1997 Umbria-Marche, Italy earthquake sequence: a first look at the mainshocks and aftershocks*. Geoph. Res. Lett., **25**, 2861-2864

Anelli L., Gorza M., Pieri M, Riva M.; 1994: *Subsurface well data in the Northern Apennines (Italy)*. Memorie Società Geologica Italiana, **48**, 461-471.

Argnani A.; 1998: *Structural elements of the Adriatic foreland and their relationships with the front of the Apennine fold-and-thrust belt*. Memorie Società Geologica Italiana, **52**, 647-654.

Barchi M., De Feyter A., Magnani M.B. et al.; 1998a: *The deformed foreland of the Northern Apennines and its structural style*. Memorie Società Geologica Italiana, **52**, 557-578.

Barchi M., Minelli G. and Pialli G.; 1998b: *The CROP 03 profile: a synthesis of results on deep structures of the northern Apennines*. Memorie Società Geologica Italiana, **52**, 383-400.

Beccaluva L., Brotzu P., Macciotta G., Morbidelli G., Serri G. and Traversa G.; 1989: *Cenozoic tectono-magmatic evolution and inferred mantle sources in the Sardo-Tyrrhenian area*. In: Boriani et al. (eds), The Lithosphere in Italy, Accad. Naz. Lincei, Roma, pp. 229-248.

Bickle M. J., Hawkesworth C.J., England P.C., and Athey D. R.; 1975: *A preliminary thermal model for regional metamorphism in the Eastern Alps*. Earth Planet. Sci. Lett., **26**, 13-28.

Boncio M., Brozzetti F., Ponziani F. et al.; 1998: *Seismicity and extensional tectonics in the Northern Umbria-Marche Apennines*. Memorie Società Geologica Italiana, **52**, 539-555.

Brewer J.; 1981: *Thermal effects of thrust faulting*. Earth Planet.Sc.Lett, **56**, 233-244.

Byerlee J.D.; 1978: *Friction of rocks*. Pure Appl. Geophys., **116**, 616-626.

Carslaw H.S. and Jaeger J.C.; 1959: *Conduction of heat in solids.* Oxford University Press, New York , 510 pp.

Castellarin A.; 1994: *Strutturazione eo-mesoalpina dell'Appennino Settentrionale attorno al "nodo ligure".* In: Capozzi R. and Castellarin A. (eds), Studi preliminari all'acquisizione dati del profilo CROP 1-1° La Spezia - Alpi orientali, Studi Geologici Camerti, Volume speciale 1992-**2**, 99-108.

Castellarin A.; 2001: *Alps - Apennines and Po Plain- frontal Apennines relations*. In: Vai G.B. and Martini I.P. (eds), Anatomy of an Orogen, Kluwer Academic Publishers, London, pp. 1-632.

Castellarin A., Eva C. and Capozzi R.; 1994: *Tomografie sismiche e interpretazione geologica profonda dell'Appennino settentrionale nord-occidentale*. Studi Geol. Camerti. Volume speciale, 1992/**2**, 85-98.

Cermak V. and Bodri L.; 1996: *Time dependent deep temperature modelling: Central Alps*. Tectonophysics, **257**, 7-24.

Channel J.E.T. and Mareschal J.C.; 1989: *Delamination and asymmetric lithospheric thickening in the development of the Tyrrhenian rift*. In: Coward M.P., Dietrich D. and Park R.G. (eds), Alpine Tectonics, Geological society, London,

Special Publications **45**, 285-302.

Collettini C., Barchi M., Pauselli C., Federico C., and Pialli G.; 2000: *Seismic expression of active extensional faults in northern Umbria (Central Italy).* Journ. Geodyn., **29**, 309-321.

Della Vedova B., Bellani S.,Pellis G. and Squarci P.; 2001: *Deep Temperatures and Surface Heat Flow Distribution.* In: Vai G.B. and Martini I.P. (eds), Anatomy of an Orogen, Kluwer Academic Publishers, London, pp. 1-632.

Doglioni C.; 1991: *A proposal of kinematic modelling for W-dipping subductions - Possible applications to the Tyrrhenian-Apennine system*. Terra Nova, **3**, 423-434.

Doglioni C., Mongelli F. and Pialli G.P.; 1998: *Boudinage of the Alpine belt in the Apenninic back-arc*. Mem. Soc. Geol. It., **52**, 457-468.

Doglioni C., Gueguen E., Harabaglia P., and Mongelli F.; 1999a: *On the origin of the west-directed subduction zones and applications to the western Mediterranean*. In: Durand B., Jolivet L., Horvath F. and Seranne M. (eds), The Mediterranean basins: Tertiary extension within the Alpine Orogen, Geological Society, London, Special Publications, **156**, 541-561.

Doglioni C., Harabaglia P., Merlini S., Mongelli F., Peccerillo A., Piromallo C.; 1999b: *Orogen and slabs vs. their direction of subduction*. Earth-Science Rev., **45**, 167-208

Dragoni M., Doglioni C., Mongelli F. and Zito G.; 1996: *Evaluation of stresses in two geodynamically different areas: stable foreland and extensional back-arc*. Pure Appl. Geophys., **146**, 319-341.

Dragoni M, Harabaglia P, and Mongelli F.; 1997: *Stress Field at a Transcurrent Plate Boundary in the Presence of frictional Heat Production at Depth*. Pure Appl. Geophys., **150**, 181-281.

England P.; 1978: *Some thermal considerations of the Alpine metamorphism past, present and future*. Tectonophysics, **6**, 21-40.

England, P. and Molnar, P.; 1990: *Surface uplift, uplift of rocks, and exhumation of rocks,* Geology, **18**, 1173-1177.

Faccenna C., Davy P., Brun J.P., Funiciello R., Giardini D., Mattei M. and Nalpas T.; 1996: *The dynamics of back-arc extension: an experimental approach to the opening of the Tyrrhenian Sea*. Geophysical Journal International, **126**, 781-795.

Frepoli A. and Amato A.; 1997: *Contemporaneous extension and compression in the Northern Apennines from earthquake fault plane solutions*. Geophysical Journal International. **129**, 368-388.

Lachenbruch, A.H.,; 1970: *Crustal temperature and heat production: implications of the linear heat flow relation.* J. Geophys. Res., **75**, 3291-3300.

Lachenbruch A.H. and Sass J.H.; 1980: *Heat flow and energetics of the SanAndreas fault zone*. J. Geophys. Res., **85**, 6185-6223.

Lachenbruch A.H. and Sass J.H.; 1992: *Heat flow from Canjon Pass, fault strength, and tectonic implications*. J. Geophys. Res., **97**, 4995-5015.

Locardi E. and Nicolich R.; 1988: *Geodinamica del tirreno e dell'Appennino Centro-Meridionale: la nuova carta della Moho*. Memorie Società Geologica Italiana. **41**, 121-140.

Loddo M., and Mongelli F.; 2005: *Palaeoclimatic effect on the temperature gradient of the Apulia*. Univ. Bari, Bari, Internal report.

Lucente P.P., Chiarabba C., Cimini G.B., and Giardini D.; 1999: *Tomographic constraints on the geodynamic evolution of the Italian region*. J. Geophys. Res., **104**, 20307-20327.

McKenzie D. and Brune J.N.; 1972: *Melting on fault planes during large earthquakes*. Geoph.J. R. Astr. Soc., **29**, 65-78.

Molnar P. and England P.; 1990: *Temperatures, heat flux, and frictional stress near major thrust faults*. J. Geophys. Res., **95**, 4833-4856.

Molnar P., Chen W.P. and Padovani E.; 1983: *Calculated temperatures in overthrust terranes and possible combination of heat sources responsible for the Tertiary granites in the greater Himalaya*. J. Geophys. Res., **88**, 6415-6429.

Mongelli F. and Pagliarulo P.; 1997: *Influence of water recharge on heat transfer in a semi-infinite aquifer*. Geothermics, **26**, 365-378.

Mongelli F., Loddo M., and Calcagnile G.; 1975: *Some observations on the Apennines gravity field*. Earth Plan. Sci.Lett., **24**, 385-393.

Mongelli F., Zito G., Ciaranfi N. and Pieri P.; 1989: *Interpretation of heat flow density on the Appennine chain, Italy*. Tectonophysics, **164**, 267-280.

Morelli A., Ekstrom G. and Olivieri M.; 2000: *Source properties of the 1997-98 Central Italy earthquake sequence from inversion of long period and broad-band seismograms*. J. of Seismology. **4**, 365-375.

Oxburgh E. R. and Turcotte D.; 1974: *Thermal gradients and regional metamorphism in overthrust terrains with special reference to eastern Alps; Schweiz*. Mineral. Petrogr. Mitt., **54**, 641-662.

Panza G.F., Pontevivo A. , Chimera G., Raykova R. and Aoudia A.; 2003: *The lithosphere-asthenosphere: Italy and surroundings.* Episodes, **26**, 169-174.

Peccerillo A.; 1985: *Roman comagmatic province (central Italy): evidence for subduction-related magma genesis*. Geology, **13**, 103-106.

Piromallo C. and Morelli A., 1997: *Imaging the Mediterranean upper mantle by P-wave travel time tomography.* Annali di Geofisica, **40**, 963-979.

Royden L. H., Patacca E. and Scandone P.; 1987: *Segmentation and configuration of subducted litho-sphere in Italy: an important control on thrust belt and foredeep basin evolution*. Geology, **15**, 714-717.

Rybach L.; 1988: *Determination of Heat Production Rate.* In: Haenel R., Rybach L. and Stegena L. (eds), Handbook of Terrestrial Heat-Flow Density Determination, Kluwer Academic Publishers, London, pp. 125-141.

Scholz C. H.; 1988: *The brittle-plastic transition and the depth of seismic faulting*. Geol. Runds. **77,** 319-328**.**

Scholz C.H.; 1990: *The mechanics of earthquakes and faulting*. Cambridge University Press, Cambridge, 439 pp.

Selvaggi G. and Chiarabba C.; 1995: *Seismicity and P-wave velocity image of the Southern Tyrrhenian subduction zone*. Geophysical Journal International, **121**, 818-826.

Serri G., Innocenti F. and Manetti P.; 1993: *Geochemical and petrological evidence of the subduction of delaminated Adriatic continental lithosphere in the genesis of the Neogene-Quaternary magmatism of Central Italy*. Tectonophysics, **223**, 117-147.

Spakman W.; 1989: *Tomographic images of the upper mantle below central Europe and the Mediterranean*. Terra Nova, **2**, 542-553.

Tallarico A., Santini S. and Dragoni M.; 2005: *Stress changes due to recent seismic events in the Central Apennines (Italy).* Pure Appl. Geophys, in press.

Zoth G. and Haenel R.; 1988: *Appendix*. In: Haenel R., Rybach L. and Stegena L. (eds), Handbook of Terrestrial Heat-Flow Density Determination, Kluwer Academic Publishers, London, pp. 449-467.

Corresponding author: Francesco Mongelli
Università di Bari
Facoltà di Scienze Matematiche Fisiche e Naturali
Via Orabona 4, 70125 Bari
phone: +39 0805442578; fax: +39 0805442625; e-mail: f.mongelli@geo.uniba.it

Appendix

During the sliding of an overthrusting block on the Lithosphere, a fraction of the work done by the friction along the sliding surface S is converted into heat; therefore, any infinitesimal element of S can be considered as an instantaneous heat source per unit area and unit time Q_c:

$$Q_c = v\tau\,, \tag{A.1}$$

where τ is the average shear stress (see the text) and v the average relative velocity of the blocks along S. The temperature field generated by instantaneous friction along a surface of sliding S located in $z=z'$, can then be found by using the image method (Carslaw and Jaeger, 1959). The result obtained is:

$$T(z,t) = \frac{q}{2\sqrt{\pi kt}}\left\{\exp\left[-\left(\frac{z-z'}{2\sqrt{kt}}\right)^2\right] - \exp\left[-\left(\frac{z+z'}{2\sqrt{kt}}\right)^2\right]\right\}, \tag{A.2}$$

where q is the strength of the source, given by:

$$q = \frac{Q_c}{\rho c} = \frac{v\tau}{\rho c} = \frac{v\tau k}{\lambda}\,, \tag{A.3}$$

In (A.3) λ is the thermal conductivity of the medium, k the thermal diffusivity, ρ the density and c the specific heat of the medium.

Let us suppose now that, along S, the sliding starts at $t'=0$ and ends at $t=t_1$. The temperature in the medium, due to the friction, at a time $t<t_1$ can be obtained by the sum of the instantaneous contributions given by (A.2), that is:

$$T(z,t) = \frac{q}{2\sqrt{\pi k}}\int_0^t \left\{\exp\left[-\left(\frac{z-z'}{2\sqrt{k(t-t')}}\right)^2\right] - \exp\left[-\left(\frac{z+z'}{2\sqrt{k(t-t')}}\right)^2\right]\right\}\frac{dt'}{\sqrt{t-t'}}\,. \tag{A.4}$$

By integrating (A.4) the following result is obtained:

$$\begin{aligned} T(z,t) &= q\sqrt{\frac{t}{\pi k}}\left\{\exp\left[-\left(\frac{z-z'}{2\sqrt{kt}}\right)^2\right] - \exp\left[-\left(\frac{z+z'}{2\sqrt{kt}}\right)^2\right]\right\} + \\ &+ \frac{q}{2k}\left[(z+z')\,erfc\frac{z+z'}{2\sqrt{kt}} - |z-z'|\,erfc\frac{|z-z'|}{2\sqrt{kt}}\right], \end{aligned} \tag{A.5}$$

and:

$$\left(\frac{\partial T}{\partial z}\right)_{z=0} = \frac{q}{k} erfc \frac{z'}{2\sqrt{kt}}. \qquad (A.6)$$

In order to compute the temperature field after the sliding for $t>t_1$, we add the virtual negative image to the real heat source. The following result is obtained:

$$\begin{aligned} T(z,t) = {} & q\sqrt{\frac{t}{\pi k}}\left\{\exp\left[-\left(\frac{z-z'}{2\sqrt{kt}}\right)^2\right]-\exp\left[-\left(\frac{z+z'}{2\sqrt{kt}}\right)^2\right]\right\}+ \\ & +\frac{q}{2k}\left[(z+z')erfc\frac{z+z'}{2\sqrt{kt}}-|z-z'|erfc\frac{|z-z'|}{2\sqrt{kt}}\right]+ \\ & -q\sqrt{\frac{t-t_1}{\pi k}}\left\{\exp\left[-\left(\frac{z-z'}{2\sqrt{k(t-t_1)}}\right)^2\right]-\exp\left[-\left(\frac{z+z'}{2\sqrt{k(t-t_1)}}\right)^2\right]\right\}+ \\ & -\frac{q}{2k}\left[(z+z')erfc\frac{z+z'}{2\sqrt{k(t-t_1)}}-|z-z'|erfc\frac{|z-z'|}{2\sqrt{k(t-t_1)}}\right], \end{aligned}$$

$$\begin{aligned} T(z,t) = {} & q\sqrt{\frac{t}{\pi k}}\left\{\exp\left[-\left(\frac{z-z'}{2\sqrt{kt}}\right)^2\right]-\exp\left[-\left(\frac{z+z'}{2\sqrt{kt}}\right)^2\right]\right\}+ \\ & -q\sqrt{\frac{t-t_1}{\pi k}}\left\{\exp\left[-\left(\frac{z-z'}{2\sqrt{k(t-t_1)}}\right)^2\right]-\exp\left[-\left(\frac{z+z'}{2\sqrt{k(t-t_1)}}\right)^2\right]\right\}+ \\ & +\frac{q}{2k}\left\{\begin{array}{l}(z+z')\left[erf\dfrac{z+z'}{2\sqrt{k(t-t_1)}}-erf\dfrac{z+z'}{2\sqrt{kt}}\right]+ \\ \qquad -|z-z'|\left[erf\dfrac{|z-z'|}{2\sqrt{k(t-t_1)}}-erf\dfrac{|z-z'|}{2\sqrt{kt}}\right]\end{array}\right\}, \end{aligned} \qquad (A.7)$$

and:

$$\left(\frac{\partial T}{\partial z}\right)_{z=0} = \frac{q}{k}\left[erfc\frac{z'}{2\sqrt{kt}}-erfc\frac{z'}{2\sqrt{k(t-t_1)}}\right] = \frac{q}{k}\left[erf\frac{z'}{2\sqrt{k(t-t_1)}}-erf\frac{z'}{2\sqrt{kt}}\right]. \qquad (A.8)$$